

Contribution from the Department of Chemistry, University of Minnesota, Minneapolis, Minnesota 55455, and the Department of Inorganic Chemistry, University of Nijmegen, Toernooiveld, 525ED Nijmegen, The Netherlands

Synthesis and Characterization of Cationic Gold-Iridium Clusters. Structure of $[\text{IrAu}_2(\text{H})(\text{PPh}_3)_4\text{NO}_3]\text{BF}_4$

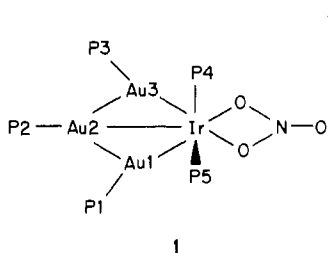
A. L. CASALNUOVO,[†] T. LASKA,[†] P. V. NILSSON,[†] J. OLOFSON,[†] L. H. PIGNOLET,^{*,†} W. BOS,[†] J. J. BOUR,[†] and J. J. STEGGERDA[†]

Received May 29, 1984

Several new cationic gold-iridium phosphine clusters have been prepared by the reaction of $\text{AuPPh}_3\text{NO}_3$ with $[\text{Ir}(\text{PPh}_3)_2(\text{H})_2(\text{acetone})_2]\text{BF}_4$ with use of acetone as solvent. At -78°C the reaction gives the doubly hydrido-bridged adduct $[(\text{acetone})_2(\text{PPh}_3)_2\text{Ir}(\mu\text{-H})_2\text{Au}(\text{PPh}_3)]^{2+}$. When it was warmed to ca. -10°C , the monohydrido Au_2Ir complex $[\text{IrAu}_2(\text{H})(\text{PPh}_3)_4\text{NO}_3]^+$ was isolated in good yield. This complex was isolated as a BF_4 salt and was characterized by single-crystal X-ray diffraction [monoclinic, $P2_1/n$ ($T = -20^\circ\text{C}$), $a = 11.931(3) \text{ \AA}$, $b = 14.472(8) \text{ \AA}$, $c = 40.97(1) \text{ \AA}$, $\beta = 91.09(2)^\circ$, $Z = 4$; $R = 0.053$ for 6276 observed reflections with $F_o^2 \geq 2\sigma(F_o^2)$]. Its structure consists of an equilateral Au_2Ir triangle with Au-Ir distances of 2.673 and 2.697 \AA and a Au-Au distance of 2.728 \AA . The nitrate group is symmetrically chelated to the Ir atom and lies approximately in the Au_2Ir plane. ^{31}P and ^1H NMR indicate that the hydride ligand is bonded to Ir in a terminal fashion. The Ir atom is therefore seven-coordinate with a distorted pentagonal-bipyramidal geometry, with trans phosphines occupying the axial positions. When an acetone solution of this compound was further warmed to 25°C , the Au_3Ir cluster $[\text{IrAu}_3(\text{PPh}_3)_5(\text{NO}_3)]^+$ formed. This entire reaction sequence has been monitored by ^{31}P and ^1H NMR spectroscopy at various temperatures. The spectroscopy, structures, and reactivity of these complexes are presented, and the mechanism of the formation of Au-Ir bonds is discussed.

Introduction

There has been considerable interest recently in the preparation and structural characterization of mixed-metal cluster compounds that contain gold atoms.¹⁻¹² Most of these clusters contain primarily carbonyl ligands bonded to the transition metals, and preparative methods have included reactions between anionic or neutral transition-metal carbonyl clusters or carbonyl hydrido clusters and monomeric gold compounds such as $\text{Au}(\text{PR}_3)\text{Cl}$ or $[\text{Au}(\text{PR}_3)]^+$. Several mixed-metal gold clusters that contain primarily phosphine ligands have been prepared by reaction of monomeric gold compounds (AuPPh_3X ; $\text{X} = \text{Cl}, \text{NO}_3$) with phosphine hydrido compounds.^{1,6,11} These reactions and the structures of the products have clearly shown the isolobal analogy between the hydride ligand and the AuPR_3 group.⁸⁻¹¹ For example, $[\text{Ir}_3(\mu_3\text{-AuNO}_3)\text{H}_6(\text{dppe})_3]^+$ and $[\text{IrAu}_3(\text{PPh}_3)_5(\text{NO}_3)]^+$ (1) have been prepared by reaction of $\text{AuPPh}_3\text{NO}_3$ with $[\text{Ir}_3\text{-}$



$(\mu_3\text{-H})\text{H}_6(\text{dppe})_3]^+$ and $[\text{Ir}_2(\mu\text{-H})_3\text{H}_2(\text{PPh}_3)_4]^+$, respectively.¹ The structure of 1 was determined by single-crystal X-ray diffraction and is unusual because it consists of a planar Au_2Ir grouping.¹

Complex 1 has been prepared in significantly better yield by reaction of $[\text{Ir}(\text{PPh}_3)_2\text{H}_2(\text{acetone})_2]\text{BF}_4$ (2) with $\text{AuPPh}_3\text{NO}_3$ in acetone solution at room temperature. This reaction has been studied at low temperature, and several bridging hydrido gold-iridium intermediates have been isolated and characterized. Gold hydrides are rare, and only a few have been previously reported.^{6,7} The structures of these intermediates give some insight into the mechanism of formation of the Au-Ir bond. The results of these studies are reported in this paper.

Mixed-metal gold clusters are important because of their potential use as catalysts and in the preparation of materials of definite composition. Our research is aimed at the synthesis of discrete mixed-metal clusters and the study of their reactivity and catalytic properties. An understanding of how the transition metal-gold bond is formed is of fundamental interest and of

importance in the design of syntheses of new clusters.

Experimental Section

Physical Measurements and Reagents. ^1H and $^{31}\text{P}\{^1\text{H}\}$ NMR spectra were recorded at 300 and 120.5 MHz, respectively, with the use of a Nicolet NT-300 spectrometer. ^{31}P chemical shifts are reported in ppm relative to the internal standard trimethyl phosphate. IR spectra were recorded on a Beckman Model 4250 grating spectrometer with the use of KBr disks. Solvents were dried and distilled prior to use. HBF_4 was obtained from the J. T. Baker Chemical Co. as a 48-50% aqueous solution. MeMgCl was obtained from the Aldrich Chemical Co. as a 2.9 M THF solution. $\text{AuPPh}_3\text{NO}_3$ ¹³ and $[\text{Ir}(\text{PPh}_3)_2\text{H}_2(\text{acetone})_2]\text{BF}_4$ ¹⁴ were prepared as described in the literature. All manipulations were carried out under a purified N_2 atmosphere with the use of standard Schlenk techniques unless otherwise noted.

Preparation of Compounds. $[\text{IrAu}_2(\text{H})(\text{PPh}_3)_4\text{NO}_3]\text{BF}_4$ (3) was prepared according to the following synthesis without the use of an inert atmosphere. $[\text{Ir}(\text{PPh}_3)_2\text{H}_2(\text{acetone})_2]\text{BF}_4$ (150 mg, 0.163 mmol) was dissolved in 2 mL of acetone and then the resultant mixture cooled to -50°C . To this colorless stirred solution was added a solution of $\text{AuPPh}_3\text{NO}_3$ (178 mg, 0.342 mmol) in 3 mL of acetone. The solution was warmed to -15°C and stirred for about 1 h during which time it gradually turned yellow. The rapid addition of 40 mL of cold Et_2O resulted in the precipitation of a flaky yellow solid that slowly changed into a fine yellow powder at -10°C . Crystallization of the yellow powder from acetone/ Et_2O solution at -20°C afforded large yellow crystals of 3 in 85% yield. This recrystallization was best carried out with a minimum amount of acetone because 3 is very soluble in acetone. Solutions of 3 decomposed slowly over several days even at -20°C . Crystals of 3 also slowly decomposed during a period of several weeks at 25°C and were best stored

[†]University of Minnesota.

[‡]University of Nijmegen.

- Casalnuovo, A. L.; Pignolet, L. H.; van der Velden, J. W. A.; Bour, J. J.; Steggerda, J. J. *J. Am. Chem. Soc.* **1983**, *105*, 5957.
- Steggerda, J. J.; Bour, J. J.; van der Velden, J. W. A. *Recl. Trav. Chim. Pays-Bas* **1982**, *101*, 164.
- Mingos, D. M. P. *Proc. R. Soc. London, Ser. A* **1982**, *308*, 75.
- Johnson, B. F. G.; Lewis, J.; Nicholls, J. N.; Puga, J.; Whitmire, K. H. *J. Chem. Soc., Dalton Trans.* **1983**, 787.
- Teo, B. K.; Keating, K. *J. Am. Chem. Soc.* **1984**, *106*, 2224.
- Lehner, H.; Matt, D.; Pregosin, P. S.; Venanzi, L. M. *J. Am. Chem. Soc.* **1982**, *104*, 6825.
- Green, M.; Orpen, A. G.; Salter, I. D.; Stone, F. G. A. *J. Chem. Soc., Chem. Commun.* **1982**, 813.
- Lauher, J. W.; Wald, K. *J. Am. Chem. Soc.* **1981**, *103*, 7648.
- Lavigne, G.; Papageorgiou, F.; Bonnet, J.-J. *Inorg. Chem.* **1984**, *23*, 609 and references therein.
- Evans, D. G.; Mingos, D. M. P. *J. Organomet. Chem.* **1982**, *232*, 171 and references therein.
- Braunstein, P.; Lehner, H.; Matt, D.; Tiripicchio, A.; Tiripicchio-Camellini, M. *Angew. Chem., Int. Ed. Engl.* **1984**, *23*, 304 and references cited therein.
- Hutton, A. T.; Pringle, P. G.; Shaw, B. L. *Organometallics* **1983**, *2*, 1889.
- Malatesta, L.; Naldini, L.; Simonetta, G.; Cariati, F. *Coord. Chem. Rev.* **1966**, *1*, 255.
- Shapley, J. R.; Schrock, R. R.; Osborn, J. A. *J. Am. Chem. Soc.* **1969**, *91*, 2816.

at temperatures below $-10\text{ }^{\circ}\text{C}$. $^{31}\text{P}\{^1\text{H}\}$ NMR (acetone- d_6 , $-90\text{ }^{\circ}\text{C}$): δ 7.3 (s, intens 2), 7.9 (s, intens 1), 35.9 (s, intens 1). ^1H (acetone- d_6 , $-90\text{ }^{\circ}\text{C}$): δ -25.3 (quint, $J_{\text{P-H}} = 13\text{ Hz}$). An elemental analysis of **3** was not obtained due to its thermal instability, but the complex was considered to be pure by ^{31}P and ^1H NMR spectroscopy. An ether solvate molecule was observed by ^1H NMR and confirmed by X-ray diffraction (vide infra).

[IrAu₂(PPh₃)₃NO₃]BF₄ (1). The synthesis has been previously reported;¹ however, an improved synthesis has since been discovered and is described here. To a suspension of 100 mg (0.056 mmol) of crushed **3** and 30 mg (0.056 mmol) of AuPPh₃NO₃ in 2 mL of THF at $0\text{ }^{\circ}\text{C}$ was added 21 μL (0.061 mmol) of 2.9 M MeMgCl solution. A very deep green solution resulted immediately. The solvent was removed in vacuo leaving a dark green residue.¹⁵ A solution of 30 mg (0.056 mmol) of AuPPh₃NO₃ in 3 mL of CH₂Cl₂ was added to the green residue. The solution was stirred for 10 min at $25\text{ }^{\circ}\text{C}$ during which time it turned to a deep red-brown. The solvent was removed in vacuo leaving a red-brown residue. The residue was redissolved in ca. 1 mL of acetone and the resultant mixture stirred for 6 h. During this time a red-brown powder precipitated from the solution. The crude product was filtered, washed with THF to remove AuPPh₃Cl, redissolved in CH₂Cl₂, and filtered again. The addition of ether to the red-brown filtrate afforded **1** as a red-brown powder in 60% yield. $^{31}\text{P}\{^1\text{H}\}$ NMR (CH₂Cl₂, $25\text{ }^{\circ}\text{C}$): δ 39.2 (t, $J = 9.5\text{ Hz}$, intens 1), 10.9 (m, intens 2), -7.25 (t, $J = 7.5\text{ Hz}$, intens 2). Anal. Calcd for IrAu₂P₃C₃₀H₇₅BF₄NO₃: C, 48.18; H, 3.37. Found: C, 47.36; H, 3.41.

Saturation Transfer Experiment. Acetone- d_6 solutions of **2**, **5**, and AuPPh₃NO₃ were generated by mixing 1 equiv of AuPPh₃NO₃ with 1 equiv of **2** at $-78\text{ }^{\circ}\text{C}$. The saturation transfer experiments were carried out on this solution at $-105\text{ }^{\circ}\text{C}$ using the Nicolet one pulse with decoupler presaturation experiment (PRESAT).¹⁶ All of the saturation transfer experiments were carried out under identical conditions, and the corresponding spectra were recorded on the same scale. The areas of the hydride resonances of **2** and **5** were measured relative to the areas of the resonances of the internal standard *p*-methoxyacetophenone.

X-ray Structure Determination. Collection and Reduction of X-ray Data. A summary of crystal and intensity data for compound **3** is presented in Table I. A crystal was secured to the end of a glass fiber with 5-min epoxy resin. Crystals of **3** were somewhat temperature sensitive so the mounted crystal was rapidly transferred to the diffractometer and maintained at $-20 \pm 3\text{ }^{\circ}\text{C}$ during centering, indexing, and data collection. The crystal class of the compound was determined by use of the Enraf-Nonius CAD 4-SDP PLUS peak search, centering, and indexing programs.¹⁷ The intensities of three standard reflections were measured every 1.5 h of X-ray exposure time. Compound **3** decayed as a linear function of X-ray exposure time. A linear correction was applied by use of program DECAY.¹⁷ The decay corrections applied were as follows: minimum 0.95; maximum 1.59; average 1.14. An empirical absorption correction was applied by use of ψ -scan data and programs PSI and EAC.¹⁷

Solution and Refinement of the Structure. The structure was solved by conventional heavy-atom techniques. The metal atom was located by Patterson syntheses. Full-matrix least-squares refinement and difference-Fourier calculations were used to locate all remaining non-hydrogen atoms. The atomic scattering factors were taken from the usual tabulation,¹⁸ and the effects of anomalous dispersion were included in F_o by using Cromer and Ibers¹⁹ values of $\Delta f'$ and $\Delta f''$. Tables of observed and calculated structure factor amplitudes are available.²⁰ Hydrogen atom positions were calculated (C-H distance set at 0.95 \AA) for all hydrogen atoms in the cation of **3** and were included in structure factor calculations but were not refined. In the crystal of compound **3** the BF₄ anion was found to be disordered. Anisotropic refinement lead to imaginary ther-

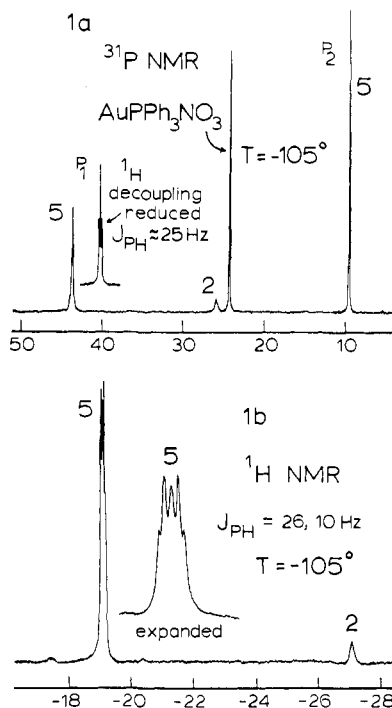


Figure 1. $^{31}\text{P}\{^1\text{H}\}$ and ^1H NMR spectra of an acetone solution of AuPPh₃NO₃ and 2 equiv of **2** recorded at $-105\text{ }^{\circ}\text{C}$. Chemical shifts are given in ppm. The insert in 1a shows the P1 resonance of **5** with the ^1H noise decoupling power reduced to reveal P hydride coupling.

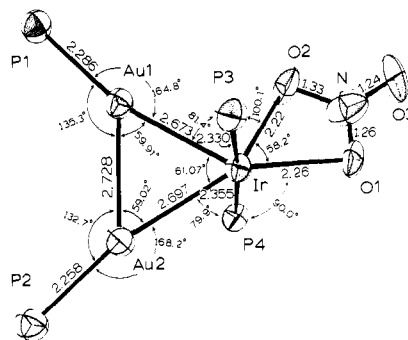


Figure 2. ORTEP drawing of the coordination core of [IrAu₂(H)(PPh₃)₄NO₃]BF₄ (**3**) including selected distances (Å) and angles (deg). The thermal ellipsoids show 50% probability surfaces. The esd's in the M-M, M-P, Ir-O, and N-O distances and the M-M-M, M-M-P, P-Ir-O, and O-Ir-O angles are 1, 4, 1, 2, 2, 1, 3, and 3, respectively, in the last significant figure. Some additional angles (deg): O2-Ir-Au1 = 88.7 (2); O2-Ir-Au2 = 144.2 (2); O1-Ir-Au1 = 145.8 (2); O1-Ir-Au2 = 152.8 (2); P3-Ir-P4 = 174.0 (1); P3-Ir-O1 = 95.3 (3); P4-Ir-O2 = 85.1 (3); P3-Ir-Au2 = 94.2 (1); P4-Ir-Au1 = 95.8 (1); Ir-O1-N = 93.6 (8); Ir-O2-N = 93.8 (8); O1-N-O2 = 114 (1); O1-N-O3 = 124 (1); O2-N-O3 = 122 (1).

mal parameters, and attempts to fit the model with additional fluorine positions were unsuccessful. The model used consisted of isotropic fluorine atoms with the B atom fixed at the center of the tetrahedron. Refinement of the fluorine positions gave a reasonable geometry (see Table S4²⁰). Infrared analysis of the crystals confirmed the presence of BF₄⁻ and the spectroscopy and chemistry were consistent with the presence of only one BF₄⁻. In addition, the presence of other BF₄⁻ groups was not apparent in the final difference Fourier map. An ethyl ether molecule was found by difference Fourier analysis and the atoms (C1, C2, C3, C4, O7) were refined in the least-squares calculations. The final difference-Fourier map did not reveal any chemically significant electron density.

The final positional and thermal parameters of the refined atoms appear in Table II and as supplementary material.²⁰ The labeling scheme is presented in Figure 2 and as supplementary material.²⁰

Results and Discussion

Synthesis and Characterization. [IrAu₂(H)(PPh₃)₄NO₃]BF₄ (**3**). The addition of 2 equiv of AuPPh₃NO₃ to [Ir(PPh₃)₂H₂(ace-

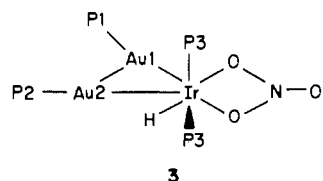
- (15) Green crystals have been isolated from this residue. Preliminary results suggest that it is the Cl⁻ analogue of **1**, [IrAu₂(PPh₃)₃Cl]⁺. ^{31}P NMR (CH₂Cl₂, $25\text{ }^{\circ}\text{C}$): 45.1 (quint, $J_{\text{P-P}} = 9.5\text{ Hz}$, intens 1), 22.9 (quart, $J_{\text{P-P}} = 9\text{ Hz}$, intens 2), -7.6 (quart, $J_{\text{P-P}} = 9\text{ Hz}$, intens 2).
- (16) PRESAT is described in the Nicolet Magnetics Corp. 1280 program manual. The following pulse and delay times were used: $D3 = 2\text{ s}$, $D4 = 100\text{ s}$, $P2 = 2\text{ s}$, $D5 = 500\text{ s}$.
- (17) All calculations were carried out on PDP 8A and 11/34 computers with use of the Enraf-Nonius CAD4 SDP-PLUS programs. This crystallographic computing package is described by: Frenz, B. A. In "Computing in Crystallography"; Schenk, H., Olthof-Hazekamp, R., van Koningsveld, H., Bassi, G. C., Eds.; Delft University Press: Delft, Holland, 1978; pp 64-71. Frenz, B. A. In "Structure Determination Package and SDP-PLUS Users Guide"; Frenz, B. A. & Associates, Inc.; College Station, TX, 1982.
- (18) Cromer, D. T.; Waber, J. T. "International Tables for X-ray Crystallography"; Kynoch Press: Birmingham, England, 1974; Vol. IV, Table 2.2.4. Cromer, D. T. *Ibid.* Table 2.3.1.
- (19) Cromer, D. T.; Ibers, J. A. Reference 18.
- (20) See paragraph at end of paper regarding supplementary material.

Table I. Summary of Crystal Data and Intensity Collection

Crystal Parameters	
formula	3·C ₂ H ₅ OC ₂ H ₅
cryst syst	monoclinic
space group	P2 ₁ /n
cryst dimens, mm ³	0.2 × 0.2 × 0.4
cell parameters	
a, Å	11.931 (3)
b, Å	14.472 (8)
c, Å	40.97 (1)
β, deg	91.09 (2)
V, Å ³	7073 (7)
Z	4
d _{calcd} , g cm ⁻³	1.75
temp, °C	-20
abs coeff, cm ⁻¹	61.5
max, min, av transmissn factors	1.0, 0.75, 0.88
molec formula	Au ₂ IrC ₇₂ H ₆₁ NO ₃ P ₄ ·BF ₄ ·C ₄ H ₁₀ O
fw	1859.3
Measurement of Intensity Data	
diffractometer	CAD 4
radiation	Mo Kα (λ = 0.710 69 Å)
	graphite monochromatized
scan type; range (2θ), deg	ω-2θ; 0-48
no. of unique reflcns	11 044 (+h, +k, ±l)
measd (region)	
no. of obsd reflcns ^a	6276 [F ₀ ² ≥ 2σ(F ₀ ²)]
Refinement by Full-Matrix Least Squares	
no. of parameters	798
R ^b	0.053
R _w ^b	0.062
GOF ^b	1.53
p ^a	0.04

^a The intensity data were processed as described in: "CAD4 and SDP-PLUS User's Manual"; B. A. Frenz & Associates, Inc.: College Station, TX, 1982. The net intensity $I = [K/NPI](C - 2B)$, where $K = 20.1166$ (attenuator factor), $NPI =$ ratio of fastest possible scan rate to scan rate for the measurement, $C =$ total count, and $B =$ total background count. The standard deviation in the net intensity is given by $[\delta(I)]^2 = (K/NPI)^2 [C + 4B + (pI)^2]$ where p is a factor used to downweight intense reflections. The observed structure factor amplitude F_o is given by $F_o = (I/LP)^{1/2}$, where $LP =$ Lorentz and polarization factors. The $\sigma(I)$'s were converted to the estimated errors in the relative structure factors $\sigma(F_o)$ by $\sigma(F_o) = 1/2 [\sigma(I)/I] F_o$. ^b The function minimized was $\sum w(|F_o| - |F_c|)^2$, where $w = 1/[\sigma(F_o)]^2$. The unweighted and weighted residuals are defined as $R = (|F_o| - |F_c|) / \sum |F_o|$ and $R_w = [(\sum w(|F_o| - |F_c|)^2) / (\sum w |F_o|)^2]^{1/2}$. The error in an observation of unit weight (GOF) is $[\sum w(|F_o| - |F_c|)^2 / (NO - NV)]^{1/2}$, where NO and NV are the number of observations and variables, respectively.

tone)₂]BF₄ (**2**) in acetone solution at -15 °C gave the cationic mixed-metal Ir-Au cluster [IrAu₂(H)(PPh₃)₄NO₃]BF₄ (**3**) in high



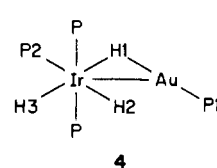
3

yield. **3** was characterized by IR and ³¹P and ¹H NMR spectroscopy, and its solid-state structure was determined by a single-crystal X-ray analysis (vide infra). **3** is believed to contain a terminal iridium hydride and to have pentagonal-bipyramidal geometry about the Ir as shown in the drawing of **3** (vide infra). The ³¹P{¹H} NMR spectrum of **3** with acetone as solvent at -90 °C is in agreement with this structure and consists of three singlets with relative intensities of 1:1:2: δ 35.9 (P₂, s, intens 1), 7.9 (P₁, s, intens 1), 7.3 (P₃, s, intens 2). P-P coupling was not resolved. Assignments of the P₁ and P₂ resonances are based upon the similarity in ³¹P NMR chemical shifts between **3** and the pre-

viously reported isolobal complex [IrAu₃(PPh₃)₅NO₃]BF₄ (**1**).¹ The presence of the hydride ligand in **3** was confirmed by the observation of a quintet resonance at -25.3 ppm ($J_{P-H} = 13$ Hz) in the ¹H NMR spectrum of **3** at -90 °C. Selective ¹H{³¹P} NMR decoupling experiments showed that the quintet resulted from a coincidental overlap of coupling constants with $J_{P_3-H} \approx J_{P_2-H} \approx J_{P_1-H} \approx 13$ Hz. However, a dynamic process that averages the P₁ and P₂ environments has been observed in the ³¹P NMR at temperatures above 25 °C (vide infra). This process is fast with respect to the ¹H NMR experiment, and therefore an average coupling constant for P₁-H and P₂-H coupling will be observed.

The bonding mode of the hydride is of particular interest. As several researchers have recently pointed out, the hydride ligand and the Au-P fragment may be considered isolobal analogues.⁸⁻¹¹ In fact, the structural similarities between the isolobal complexes **3** and **1** are striking (vide infra) and suggest the possibility that the hydride in **3** may be bridging the Ir-Au₂ bond. Unfortunately, a completely unambiguous assignment of the hydride position in **3** has not proved possible. Although the absence of a terminal Ir-H stretch in the infrared spectrum of **3** does not provide support for a terminal bonding mode,²¹ the magnitude of J_{AuP-H} is most consistent with a terminal hydride formulation.^{6,7}

Examples of stable, mixed transition metal-gold complexes containing gold hydride interactions are rare, and only two examples have recently been reported.^{6,7} In both cases, the gold-phosphine bond was found to be approximately trans to the bridging hydride rather than to the transition metal. The Ir-Au complex [Ir(PPh₃)₃H₂(μ-H)AuPPh₃]BF₄ (**4**) reported by Venanzi



4

et al.⁶ is particularly relevant since it contains both bridging and terminal hydrides as shown in the drawing. Consistent with their orientation, a spin-spin coupling constant of 79 Hz was observed between the gold phosphine P₁ and the bridging hydride H₁ in this complex.²² The coupling constant observed between the gold phosphine P₁ and the terminal hydride H₂ was much smaller (13 Hz) and in good agreement with the coupling constant observed in **3**. The P-H coupling data, therefore, suggests that **3** contains a terminal hydride. In addition, the -25.3 ppm chemical shift of the hydride in **3** is more consistent with a terminal hydride bonding mode than with a bridging one in polyhydride iridium phosphine clusters.²³ However, the use of hydride chemical shifts to assign their bonding mode must be used with caution.²⁴

³¹P{¹H} NMR spectra were recorded as a function of temperature (-90 to +90 °C) for an acetone solution of **3** to which 1 equiv of **2** had been added. As the temperature was increased, the resonances due to P₁ and P₂ broadened and coalesced at about 25 °C. The averaged P₁,P₂ resonance sharpened at higher temperatures up to 90 °C. Although some decomposition was noted at higher temperatures (new peaks at 42.8 and 20 ppm and a decrease in the signal due to **2**), the coalescence of the P₁ and P₂ resonances was reversible since the original shifts were observed when the same solution was cooled to -90 °C. This result shows that a dynamic process is occurring that interchanges the P₁ and P₂ environments. An intermolecular exchange with AuPPh₃⁺ is ruled out because the presence of added AuPPh₃NO₃ had no effect on the ³¹P NMR spectra of **3** or AuPPh₃NO₃ at different temperatures. The most likely intramolecular exchange process in-

- (21) Examples of transition-metal hydride complexes where the terminal ν_{Ir-H} is very weak or not observed are known: Kaesz, H. D.; Saillant, R. B. *Chem. Rev.* **1972**, *72*, 231.
- (22) The correlation between the P-M-H angle and J_{P-H} is well-known (see ref 21). The magnitude of J_{P-H} here is a result of both the H₁-Au bonding interaction and the 180° P₁-Au-H₁ angle.
- (23) Wang, H. H.; Pignolet, L. H. *Inorg. Chem.* **1980**, *19*, 1470.
- (24) See ref in footnote 21.

Table II. Table of Positional Parameters and Their Estimated Standard Deviations for 3

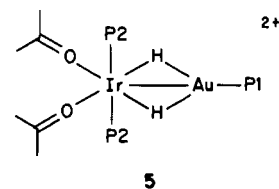
atom	x	y	z	$B, \text{\AA}^2$	atom	x	y	z	$B, \text{\AA}^2$
Ir	0.45775 (6)	0.03308 (4)	0.11598 (1)	2.54 (1)	C2F	0.580 (2)	0.435 (1)	0.2169 (4)	5.2 (5)
Au1	0.47420 (6)	0.19920 (5)	0.08798 (2)	2.90 (1)	C3F	0.653 (2)	0.510 (2)	0.2114 (5)	7.0 (6)
Au2	0.45148 (6)	0.18522 (5)	0.15393 (1)	2.88 (1)	C4F	0.682 (2)	0.528 (1)	0.1819 (6)	5.8 (6)
P1	0.4877 (4)	0.3184 (3)	0.0517 (1)	3.1 (1)	C5F	0.639 (2)	0.482 (1)	0.1554 (5)	6.0 (6)
P2	0.4377 (4)	0.2917 (3)	0.1939 (1)	3.2 (1)	C6F	0.567 (2)	0.409 (1)	0.1599 (5)	4.8 (5)
P3	0.6517 (4)	0.0376 (3)	0.1103 (1)	2.92 (9)	C1G	0.708 (1)	0.053 (1)	0.0702 (4)	3.4 (4)
P4	0.2639 (4)	0.0420 (3)	0.1253 (1)	2.83 (9)	C2G	0.825 (2)	0.050 (2)	0.0652 (5)	7.6 (7)
O1	0.442 (1)	-0.1210 (7)	0.1075 (3)	3.5 (3)	C3G	0.863 (2)	0.064 (2)	0.0348 (5)	9.7 (8)
O2	0.407 (1)	-0.0246 (8)	0.0677 (3)	3.9 (3)	C4G	0.794 (2)	0.070 (2)	0.0069 (5)	7.7 (6)
N	0.411 (1)	-0.112 (1)	0.0780 (3)	5.2 (4)	C5G	0.681 (2)	0.070 (1)	0.0114 (4)	5.8 (6)
O3	0.391 (1)	-0.1774 (8)	0.0594 (3)	6.9 (4)	C6G	0.638 (2)	0.060 (1)	0.0425 (4)	4.4 (5)
C1A	0.390 (1)	0.300 (1)	0.0174 (4)	3.5 (4)	C1H	0.719 (1)	0.131 (1)	0.1351 (4)	3.5 (4)
C2A	0.323 (2)	0.375 (1)	0.0046 (5)	4.6 (5)	C2H	0.708 (2)	0.125 (1)	0.1684 (4)	4.0 (4)
C3A	0.251 (2)	0.360 (1)	-0.0215 (4)	4.8 (5)	C3H	0.763 (2)	0.192 (2)	0.1866 (5)	6.8 (6)
C4A	0.241 (2)	0.272 (1)	-0.0345 (5)	5.1 (5)	C4H	0.812 (2)	0.271 (2)	0.1713 (6)	7.0 (6)
C5A	0.308 (2)	0.203 (2)	-0.0224 (4)	5.4 (5)	C5H	0.817 (2)	0.274 (2)	0.1398 (6)	7.9 (7)
C6A	0.378 (1)	0.216 (1)	0.0031 (4)	3.6 (4)	C6H	0.770 (2)	0.206 (1)	0.1201 (5)	5.1 (5)
C1B	0.626 (2)	0.331 (1)	0.0337 (4)	3.7 (4)	C1I	0.727 (1)	-0.068 (1)	0.1244 (4)	3.6 (4)
C2B	0.641 (2)	0.322 (1)	0.0010 (4)	4.4 (5)	C2I	0.821 (2)	-0.058 (2)	0.1433 (6)	6.8 (6)
C3B	0.749 (2)	0.336 (2)	-0.0123 (5)	6.4 (6)	C3I	0.876 (2)	-0.142 (2)	0.1529 (6)	7.8 (7)
C4B	0.834 (2)	0.356 (2)	0.0073 (5)	6.4 (6)	C4I	0.842 (2)	-0.226 (1)	0.1419 (5)	5.8 (5)
C5B	0.817 (2)	0.368 (2)	0.0413 (6)	6.6 (6)	C5I	0.752 (2)	-0.228 (1)	0.1221 (5)	5.2 (5)
C6B	0.713 (1)	0.356 (1)	0.0538 (4)	4.2 (4)	C6I	0.690 (2)	-0.152 (1)	0.1133 (4)	4.2 (4)
C1C	0.454 (2)	0.433 (1)	0.0689 (4)	3.4 (4)	C1J	0.217 (1)	0.041 (1)	0.1679 (4)	2.8 (3)
C2C	0.516 (2)	0.508 (1)	0.0619 (4)	4.9 (5)	C2J	0.290 (2)	0.030 (2)	0.1943 (4)	5.5 (5)
C3C	0.485 (2)	0.591 (1)	0.0747 (5)	5.6 (5)	C3J	0.252 (2)	0.026 (1)	0.2263 (4)	5.0 (5)
C4C	0.387 (2)	0.602 (1)	0.0930 (5)	5.9 (6)	C4J	0.136 (2)	0.040 (1)	0.2315 (5)	5.6 (5)
C5C	0.325 (2)	0.523 (1)	0.0991 (5)	5.1 (5)	C5J	0.068 (2)	0.056 (1)	0.2056 (4)	4.8 (5)
C6C	0.359 (2)	0.437 (1)	0.0882 (4)	4.9 (5)	C6J	0.103 (2)	0.055 (1)	0.1744 (4)	4.9 (5)
C1D	0.458 (1)	0.243 (1)	0.2345 (4)	3.2 (4)	C1K	0.198 (1)	0.140 (1)	0.1056 (4)	3.4 (4)
C2D	0.518 (2)	0.161 (1)	0.2382 (4)	4.3 (5)	C2K	0.152 (2)	0.214 (1)	0.1225 (4)	4.3 (4)
C3D	0.532 (2)	0.124 (1)	0.2693 (5)	6.2 (5)	C3K	0.109 (2)	0.285 (2)	0.1060 (5)	6.2 (6)
C4D	0.490 (2)	0.167 (2)	0.2962 (4)	6.8 (6)	C4K	0.108 (2)	0.296 (1)	0.0728 (5)	5.1 (5)
C5D	0.429 (2)	0.242 (2)	0.2918 (5)	6.3 (6)	C5K	0.154 (1)	0.220 (1)	0.0559 (5)	5.4 (5)
C6D	0.413 (2)	0.284 (1)	0.2623 (4)	4.7 (5)	C6K	0.202 (1)	0.148 (1)	0.0718 (4)	4.4 (4)
C1E	0.300 (1)	0.345 (1)	0.1950 (4)	3.2 (4)	C1L	0.185 (1)	-0.057 (1)	0.1102 (4)	3.4 (4)
C2E	0.276 (2)	0.431 (2)	0.1807 (4)	5.3 (5)	C2L	0.207 (2)	-0.141 (1)	0.1251 (4)	3.8 (4)
C3E	0.166 (2)	0.458 (2)	0.1789 (5)	6.1 (6)	C3L	0.151 (2)	-0.225 (1)	0.1136 (5)	5.4 (5)
C4E	0.080 (1)	0.407 (1)	0.1911 (5)	5.0 (5)	C4L	0.074 (2)	-0.216 (2)	0.0884 (5)	6.0 (6)
C5E	0.101 (2)	0.330 (1)	0.2062 (6)	5.8 (6)	C5L	0.046 (2)	-0.135 (1)	0.0744 (5)	5.2 (5)
C6E	0.212 (2)	0.295 (1)	0.2071 (5)	4.8 (5)	C6L	0.103 (2)	-0.057 (1)	0.0850 (4)	4.0 (4)
C1F	0.536 (1)	0.386 (1)	0.1896 (4)	3.0 (4)					

^a Anisotropically refined atoms are given in the form of the isotropic equivalent thermal parameter defined as $1/3[a^2\beta_{1,1} + b^2\beta_{2,2} + c^2\beta_{3,3} + ab(\cos\gamma)\beta_{1,2} + ac(\cos\beta)\beta_{1,3} + bc(\cos\alpha)\beta_{2,3}]$.

volves the movement of the hydride to the Au1 side of the Au₂Ir triangle accompanied by a rotation of the nitrate group around an Ir-O bond.²⁵ The transition state would presumably contain a hydride that is triply bridging the Au₂Ir triangle. Examples of $\mu_3\text{-H-M}_3$ clusters are known.²³ An alternate explanation for the dynamic behavior of **3** is the rotation of the P-Au-Au-P unit about the axis that contains its midpoint and the Ir atom. The analogy between $\eta^2\text{-Au}_2\text{P}_2$ and alkyne fragments has recently been made.¹¹ The actual dynamic process may be more complex than described because broadening was also noted in the ³¹P resonance of the P3 atoms and in the ¹H hydride resonance as the temperature was increased. This broadening cannot be due to the process described above. At high temperature these resonances sharpened up. Although more work is needed in order to fully understand this result, it is likely that an isomer of **3** exists that becomes more stable at higher temperature and that interconverts with **3**.

Although a number of mixed transition metal-gold complexes have been reported, little is known about how they form. In order to gain some mechanistic insight into the formation of **3**, the reaction of AuPPh₃NO₃ with **2** was carried out at low temperature and was monitored with use of variable-temperature ³¹P{¹H} and ¹H NMR spectroscopy. These experiments have led to the identification of three Ir-H-Au-bridged intermediates.

The addition of AuPPh₃NO₃ to **2** in acetone solution at -78 °C resulted, initially, in the reversible formation of the binuclear Au-Ir adduct [Ir(PPh₃)₂(acetone)₂($\mu\text{-H}$)₂AuPPh₃]²⁺ (**5**). ¹H and

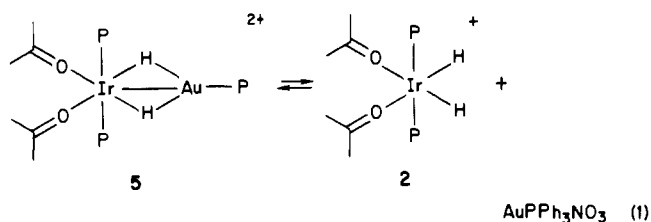


³¹P{¹H} NMR spectra of this solution showed the appearance of new signals due to the formation of the binuclear complex **5**. The NMR spectra of this solution are shown in Figure 1. The ³¹P NMR spectrum of **5** recorded at -105 °C (Figure 1a) showed two singlets with relative intensities of 2:1, attributable to P2 and P1, respectively: δ 43.5 (P1, s, intens 1), 9.49 (P2, s, intens 2). P-P coupling was not resolved. The ¹H NMR spectrum of **5** recorded at -105 °C (Figure 1b) showed a single hydride environment (δ 19.2 (m due to d of t)), which is consistent with the overall C_{2v} symmetry proposed for **5**. Selective decoupling of the ³¹P environments showed that this doublet of triplet resonance results from H-P coupling to one phosphorus atom P1 ($J = 26$ Hz) and to two equivalent phosphorus atoms P2 ($J = 10$ Hz). Additionally, selective ³¹P{¹H} NMR decoupling experiments confirmed the presence of two equivalent bridging hydrides. The magnitude of these coupling constants is also consistent with the structure shown for **5**. When the ¹H noise decoupling power was

(25) A dissociative equilibrium between AuPPh₃⁺ and [Au₂(PPh₃)₂]³⁺ has been noted previously: van der Velden, J. W. A.; Bour, J. J.; Bosman, W. P.; Noordik, J. H. *J. Chem. Soc. Chem. Commun.* **1981**, 1218.

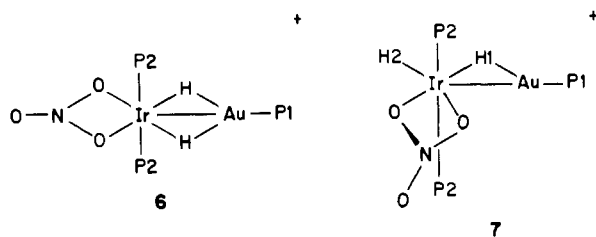
turned down, the ^{31}P resonance at δ 43.5 (assigned to P1) appeared as a triplet with $J_{\text{P-H}}$ 26 Hz (Figure 1a inst). The H coupling to the P2 phosphorus atoms was too small to be resolved. In contrast to **3**, the observation of a spin-spin coupling constant of 26 Hz between the two equivalent hydride ligands and P1 is consistent with the formation of a Au-H bond. In comparison to the previously reported Ir-H-Au complexes,^{6,7} the smaller coupling constant observed between the gold phosphine phosphorus atom and the bridging hydrides in **5** is consistent with a decreased P-Au-H angle. Recall that in **4** $J_{\text{P-H}} = 79$ Hz for trans P-Au-H stereochemistry.⁶

The formation of **5** is reversible, and an equilibrium distribution of **5**, $\text{AuPPh}_3\text{NO}_3$, and **2** has been observed by ^{31}P and ^1H NMR spectroscopy in acetone solutions of **5** at -105°C (Figure 1).²⁵ Although significant line broadening occurs in the ^{31}P and ^1H resonances of these three species upon warming solutions of **5**, the irreversible formation of new complexes (vide infra) prevents the observation of a coalescence due to rapid exchange. Fortunately, saturation transfer techniques are particularly well suited to studying equilibrium systems involving unstable species.²⁶ In the saturation transfer experiment, saturation of one of two chemical sites undergoing exchange results in a transfer of saturation to the second site and a decrease in the intensity of its resonance line. In this case, saturation transfer experiments provided unequivocal evidence for the equilibrium shown in eq 1. Saturation of the hydride resonance of **2** (δ -27.2) resulted



in a $52 \pm 2\%$ reduction of the hydride resonance of **5**. Conversely, saturation of the hydride resonance of **5** (δ -19.2) resulted in a $80 \pm 2\%$ reduction of the hydride resonance of **2**. The details of this experiment are given in the Experimental Section.

Acetone solutions of **5** reacted further upon warming, and at -35°C two new binuclear Au-Ir species, **6** and **7**, were detected.



$^{31}\text{P}\{^1\text{H}\}$ and ^1H NMR spectra (included as supplementary material)²⁰ suggest that the two complexes are isomers with the overall formulation $[\text{IrAu}(\text{PPh}_3)_3\text{H}_2\text{NO}_3]^+$. Both **6** and **7** are formed irreversibly, and no evidence for an equilibrium between the two species was found. Thus, the relative amounts of **6** and **7** are kinetically controlled. The structures proposed for **6** and **7** are shown.

The $^{31}\text{P}\{^1\text{H}\}$ and ^1H NMR spectra of the major isomer **6** are very similar to the spectra of **5** and are consistent with the displacement of coordinated acetone by NO_3^- . ^{31}P NMR: δ 44.8 (P1, s, intens 1), 5.14 (P2, s, intens 2). ^1H NMR: δ 17.5 (d of t, $J_{\text{P1-H}} = 30$, $J_{\text{P2-H}} = 10$ Hz). Again, selective $^{31}\text{P}\{^1\text{H}\}$ NMR decoupling experiments confirmed the presence of two equivalent hydrides. As with **5**, the observation of a 30-Hz coupling constant between the hydrides and the gold phosphine phosphorus atom is consistent with a bridging hydride formulation. The coordination

of the NO_3^- ligand to the Ir atom has been confirmed indirectly by monitoring the reaction of $\text{AuPPh}_3\text{NO}_3$ with the nitrate analogue of **2**,²⁷ $\text{Ir}(\text{PPh}_3)_2\text{H}_2\text{NO}_3$, in CH_2Cl_2 solution at low temperature. This reaction resulted in the complete and exclusive formation of **6** as evidenced by ^{31}P and ^1H NMR spectroscopy.²⁸

The nitrate apparently plays a major role in thermodynamically driving the reaction forward. The AuPPh_3^+ moiety is irreversibly bound upon coordination of NO_3^- to Ir. Recall that in acetone solutions of **5** the AuPPh_3^+ group is labile (vide supra). This stabilization is presumably due to the net reduction in charge that occurs when the anion is coordinated.

The minor isomer, **7**, contains two nonequivalent hydride ligands as indicated by ^1H NMR spectroscopy: δ -17.9 (H1, $J_{\text{H-P1}} = 32$, $J_{\text{H-P2}} = 10$, $J_{\text{H-H}} = 9$ Hz), -20.9 (H2, br, unresolved). The observation of a spin-spin coupling constant of 32 Hz between H1 and P1 suggests that only one hydride, H1, bridges the Ir-Au bond. No large coupling to H2 was observed. The ^{31}P NMR spectrum of **7** is consistent with the formation of a binuclear complex and resembles spectra of both **5** and **6**. The presence of and the coordination mode of the nitrate in **7** is speculative. It is noteworthy, however, that **7** is also formed irreversibly, suggesting that the nitrate is coordinated.

Further warming of acetone solutions of **6** and **7** to ca. -10°C resulted in the quantitative formation of **3** when 2 equiv of $\text{AuPPh}_3\text{NO}_3$ were initially used. Additional intermediates were not detected. Other, as yet, unidentified minor species were detected, however, when less than 2 equiv of $\text{AuPPh}_3\text{NO}_3$ were used. Attempts to identify these compounds are currently in progress. Acetone solutions of **3** were stable at temperatures below -20°C ; however, slow decomposition into **1** occurred at room temperature (vide infra).

Acetone solutions of **3**, although stable to air, were thermally unstable and decomposed slowly over several days at room temperature to form **1** in about 35-40% yield. Two other species were detected as a result of this decomposition by ^{31}P NMR spectroscopy, but they were not identified. Surprisingly, the addition of $\text{AuPPh}_3\text{NO}_3$ to an acetone solution of **3** did not result in an increased yield of **1**. Significantly higher yields (60%) of **1** were obtained when **3** was treated with a THF solution of MeMgCl at 25°C in the presence of $\text{AuPPh}_3\text{NO}_3$. This reaction is also fast, but the nature of the interaction is not understood and continued work on this reaction is needed.

Preliminary investigations into the reactivity of these Ir-Au clusters with small molecules such as H_2 and CO have been initiated. Acetone solutions of **3** and **1**, for example, reacted rapidly with H_2 (1 atm) at room temperature to give new hydride species. Initial results suggest that the hydrogenation of **1** produced a larger mixed-metal cluster with an overall formulation of $[\text{IrAu}_4(\text{PPh}_3)_6(\text{H})_2]^+$.

These reactivities are interesting and suggest that the Au-Ir clusters may be potential catalysts. The details of these reactivity studies will be published when completed, and the usefulness of these materials as catalysts is being examined.

X-ray Structure Determination. $[\text{IrAu}_2(\text{H})(\text{PPh}_3)_4\text{NO}_3]\text{BF}_4 \cdot (\text{C}_2\text{H}_5)_2\text{O}$ (**3**). The structure of **3** consists of discrete cations, anions, and ether solvate molecules. There are no unusually short contacts between these species. Figure 2 shows an ORTEP drawing

(26) Faller, J. W. In "Determination of Organic Structures by Physical Methods"; Nachod, F., Zukerman, J., Eds.; Academic Press: New York, 1973; Vol. 5. Tolman, C. A.; Faller, J. W. In "Homogeneous Catalysis with Metal Phosphine Complexes"; Pignolet, L. H., Ed.; Plenum Press: New York, 1983; Chapter 2.

(27) $\text{IrP}_2\text{H}_2\text{NO}_3$ was prepared from $[\text{IrP}_2\text{H}_2(\text{acetone})_2]\text{BF}_4$ by the addition of an acetone slurry of pulverized ammonium nitrate.

(28) Crystals of $[\text{IrAu}(\text{PPh}_3)_3\text{H}_2\text{NO}_3]$ (**6**) have been isolated by the solvent layering technique with use of CH_2Cl_2 and diethyl ether at -80°C . Although the crystals are of good quality, they are thermally unstable and they contain CH_2Cl_2 of crystallization, which rapidly escapes upon removal from the solvent, causing total fracturing of the crystals. This combination of problems has thwarted numerous attempts to collect X-ray diffraction data; however, accurate unit cell parameters have been determined: -125°C , triclinic, $a = 12.223$ (7) Å, $b = 14.70$ (1) Å, $c = 17.21$ (2) Å, $\alpha = 95.79$ (9)°, $\beta = 100.53$ (7)°, $\gamma = 101.16$ (6)°, $V = 2954$ Å³. Assuming a disolvate formulation $\text{Au}_1\text{Ir}_1\text{C}_{34}\text{H}_{47}\text{N}_2\text{O}_6\text{P}_3 \cdot 2\text{CH}_2\text{Cl}_2$ and $Z = 2$, these cell constants give a calculated density of 1.66 g cm⁻³, which is in good agreement with the calculated density of **3** (1.75 g cm⁻³). These data support the formulation of **6**.

(29) Casalnuovo, A. L.; Laska, T.; Nilsson, P. V.; Olofson, J.; Pignolet, L. H. *Inorg. Chem.*, companion paper in this issue.

of the $\text{IrAu}_2\text{P}_4\text{NO}_3$ core and includes atom labels and selected distances and angles. An ORTEP drawing of the entire cation and a table of all distances and angles are included as supplementary material.²⁰

The most striking feature about the structure of the cation of **3** is its similarity to the structure of **1**, with one AuPPh_3 group missing.¹ The isolobal analogy^{8–11} between H and AuPPh_3 suggests that a bridging hydride has replaced Au3; however, a careful examination of the structure of **3** indicates that a terminal iridium hydride formulation may be better (vide infra). The structure of the cation consists of an approximately equilateral IrAu_2 triangle. The Ir–Au distances are similar and are short (average 2.685 (1) Å) but are comparable to Ir–Au separations in the other known mixed-metal phosphine cluster complexes **1** (average 2.641 (1) Å)¹ and $[\text{Ir}_3(\mu_3\text{-AuNO}_3)\text{H}_6(\text{dppe})_3]^+$ (average 2.705 (1) Å).¹ The Ir–Au distance in the hydride-bridged complex **4** (2.765 (1) Å)⁶ is significantly longer, however. The lengthening of the Ir–Au separation in this bimetallic complex could be the result of the hydride bridge, especially since the Ir–Au distance in the only other known bimetallic Ir–Au complex $[\text{Ir}(\text{dppe})_2\text{AuPPh}_3](\text{BF}_4)_2$ ²³ is quite short (2.625 (1) Å) (vide infra). This latter complex does not contain a hydride bridge. This trend in Ir–Au distances must be considered tenuous at this time because there are so few Ir–Au complexes known. However, the shortness and similarity of the two Ir–Au distances in **3** suggest that the hydride ligand is bonded to Ir in a terminal fashion. Unfortunately, the hydride was not located in the final difference Fourier map. The Au–Au separation in **3** (2.728 (1) Å) is typical of other gold phosphine clusters² and is similar to the value of 2.767 (1) Å found in **1**.¹ The angles about Au1 and Au2 are very similar to those about Au1 and Au3 in **1**.¹

The atoms P1, P2, and O1 are approximately within the IrAu_2 plane (deviations of 0.044 (5), 0.058 (5), and 0.14 (1) Å, respectively) while O2 is displaced 0.76 (1) Å in the direction of P4. The P3 and P4 atoms are displaced –2.272 (4) and 2.263 (4) Å, respectively, from the plane of the IrAu_2 triangle, and these atoms have trans stereochemistry with respect to Ir (P3–Ir–P4 = 174.0 (1)°). The P3–Ir and P4–Ir vectors are approximately orthogonal to the IrAu_2 plane. The Au–P and Ir–P distances in **3** (average 2.272 (4) and 2.343 (4) Å, respectively) are similar to values found in **1** (average 2.266 (4) and 2.329 (4) Å, respectively)¹ and **4** (2.265 (5) Å and average for trans phosphines 2.330 (6) Å, respectively).⁶

The nitrate group in **3** is planar within experimental error, and the Ir atom is displaced only 0.013 (1) Å from this least-squares

plane. The dihedral angle between the NO_3 plane and the IrAu_2 plane is 22°. The Ir–O and N–O distances (average 2.24 (1) and 1.28 (2) Å, respectively) are similar to the values found in **1** (average 2.29 (1) and 1.26 (2) Å, respectively).¹

The two Ir–O distances in **3** are the same within experimental error. This is most consistent with a terminal iridium hydride stereochemistry because a bridging hydride structure (Ir–H–Au2) would place the hydride in a position approximately trans to O2, and therefore the Ir–O2 bond should be lengthened relative to the Ir–O1 distance. O1 is approximately trans to the midpoint of the Au–Au vector (O1–Ir–Au1 = 145.8 (2)°, O1–Ir–Au2 = 152.8 (2)°). It is well-known that distances to ligands that are approximately trans to bridging hydrides are significantly lengthened via the large trans influence of a metal hydride.²⁴ A terminal iridium hydride would most likely be positioned at a point that is nearly within the plane that contains the IrAu_2 and NO_3 groups and such that the Ir–H vector is approximately orthogonal to the vectors between Ir and P3, P4, O1, and Au2. This placement would result in O2–Ir–H and Au1–Ir–H angles of approximately 135°. Since this angle is significantly away from 180°, a lengthening of the Ir–O2 and Ir–Au1 bonds relative to Ir–O1 and Ir–Au2 is expected to be minimal and indeed this is the case. The above argument assumes a certain placement of the terminal hydride. Careful examination of an accurately constructed model supports this placement. It should be recalled that the ¹H NMR results (vide supra) also support a terminal hydride stereochemistry.

The distances and angles within the triphenylphosphine ligands and the BF_4^- anion are normal and are included as supplementary material.²⁰

Acknowledgement is made to the National Science Foundation (NSF Grant CHE-81-08490) and to NATO for a travel grant. The Johnson-Matthey Co. is acknowledged for a generous loan of IrCl_3 . A.L.C. is the recipient of an NSF Graduate Fellowship.

Registry No. **1**, 93895-69-3; **2**, 82582-67-0; **3**, $\text{C}_2\text{H}_5\text{OC}_2\text{H}_5$, 93895-72-8; **4**, 83527-81-5; **5**, 93895-73-9; **6**, $2\text{CH}_2\text{Cl}_2$, 93895-76-2; **7**, 93895-77-3; $[\text{IrAu}_3(\text{PPh}_3)_5\text{Cl}]^+$, 93922-98-6; $\text{AuPPh}_3\text{NO}_3$, 14897-32-6; Ir, 7439-88-5; Au, 7440-57-5.

Supplementary Material Available: Figures giving ³¹P and ¹H NMR spectra of **6** and **7** and the molecular structure of **3** and tables of positional and thermal parameters, distances and angles, least-squares planes, calculated hydrogen positional parameters, and observed and calculated structure factor amplitudes for **3** (46 pages). Ordering information is given on any current masthead page.